Physics Letters A 379 (2015) 2030–2036

Contents lists available at ScienceDirect

Physics Letters A

www.elsevier.com/locate/pla

A chaotic system with a single unstable node

J.C. Sprott [a], Sajad Jafari [b,*], Viet-Thanh Pham [c], Zahra Sadat Hosseini [b]

[a] Department of Physics, University of Wisconsin, Madison, WI 53706, USA
[b] Biomedical Engineering Department, Amirkabir University of Technology, Tehran 15875-4413, Iran
[c] School of Electronics and Telecommunications, Hanoi University of Science and Technology, 01 Dai Co Viet, Hanoi, Viet Nam

ARTICLE INFO

Article history:
Received 19 October 2014
Received in revised form 27 April 2015
Accepted 16 June 2015
Available online 19 June 2015
Communicated by A.P. Fordy

Keywords:
Chaotic flows
Unstable node
Coexisting attractors
Hidden attractors
Symmetry breaking

ABSTRACT

This paper describes an unusual example of a three-dimensional dissipative chaotic flow with quadratic nonlinearities in which the only equilibrium is an unstable node. The region of parameter space with bounded solutions is relatively small as is the basin of attraction, which accounts for the difficulty of its discovery. Furthermore, for some values of the parameters, the system has an attracting torus, which is uncommon in three-dimensional systems, and this torus can coexist with a strange attractor or with a limit cycle. The limit cycle and strange attractor exhibit symmetry breaking and attractor merging. All the attractors appear to be hidden in that they cannot be found by starting with initial conditions in the vicinity of the equilibrium, and thus they represent a new type of hidden attractor with important and potentially problematic engineering consequences.

© 2015 Elsevier B.V. All rights reserved.

1. Introduction

Most familiar examples of low-dimensional chaotic flows occur in systems having one or more saddle points. Such saddle points allow homoclinic and heteroclinic orbits and the prospect of rigorously proving the chaos when the Shilnikov condition is satisfied. Furthermore, such saddle points provide a means for locating any strange attractors by choosing an initial condition on the unstable manifold in the vicinity of the saddle point. Such attractors have been called "self-excited," and they are overwhelmingly the most common type described in the literature.

Recently, many new chaotic flows have been discovered that are not associated with a saddle point, including ones without any equilibrium points, with only stable equilibria, or with a line containing infinitely many equilibrium points [1–10]. The attractors for such systems have been called "hidden attractors" [11–17], and that accounts for the difficulty of discovering them since there is no systematic way to choose initial conditions except by extensive numerical search. Hidden attractors are important in engineering applications because they allow unexpected and potentially disastrous responses to perturbations in a structure like a bridge or aircraft wing.

Here we introduce a new class of hidden attractor that occurs in a system in which the only equilibrium is an unstable node, and we identify what may be the simplest example of such a system with a strange attractor. By "unstable node" we mean an equilibrium point whose eigenvalues are all real and positive. The system was found by extensive numerical search and appears to be extremely rare in the class of system studied, but it has a number of interesting and unusual properties including symmetry breaking, attractor merging, and multistability, as well as an attracting torus.

Section 2 describes the numerical search procedure, and Section 3 describes the properties of the equilibrium point. Section 4 shows the variety of different dynamics and their bifurcations. Section 5 illustrates examples of coexisting attractors, and Section 6 provides the evidence that these attractors are hidden. Finally, Section 7 gives the conclusions.

2. Numerical search

Perhaps the simplest chaotic flow with a single equilibrium point is a jerk system, the most general quadratic form of which is given by

$$\begin{aligned}\dot{x} &= y\\ \dot{y} &= z\\ \dot{z} &= f(x,y,z) = a_1x + a_2y + a_3z + a_4y^2\\ &\quad + a_5z^2 + a_6xy + a_7xz + a_8yz + a_9\end{aligned} \tag{1}$$

* Corresponding author.
E-mail address: sajadjafari@aut.ac.ir (S. Jafari).

http://dx.doi.org/10.1016/j.physleta.2015.06.039
0375-9601/© 2015 Elsevier B.V. All rights reserved.

System (1) has only one equilibrium point at $(-\frac{a_9}{a_1}, 0, 0)$ with eigenvalues λ that satisfy

$$\lambda^3 - f_z\lambda^2 - f_y\lambda - f_x = 0 \tag{2}$$

where $f_x = a_1$, $f_y = a_2 - a_6a_9/a_1$, and $f_z = a_3 - a_7a_9/a_1$. Since the Routh–Hurwitz stability criterion gives the conditions for having the real part of all eigenvalues negative, a transformation of Eq. (2) with $\lambda \to -\lambda$ gives the conditions for having them all positive. Thus Eq. (2) becomes $-\lambda^3 - f_z\lambda^2 + f_y\lambda - f_x = 0$, which after multiplying by -1 gives

$$\lambda^3 + f_z\lambda^2 - f_y\lambda + f_x = 0 \tag{3}$$

Thus the conditions for the equilibrium to be unstable are $f_z > 0$, $f_x + f_yf_z < 0$, and $f_x > 0$, or

$$\left(a_3 - \frac{a_7a_9}{a_1}\right) > 0$$
$$a_1 + \left(a_2 - \frac{a_6a_9}{a_1}\right)\left(a_3 - \frac{a_7a_9}{a_1}\right) < 0$$
$$a_1 > 0 \tag{4}$$

An extensive numerical search involving millions of random combinations of the coefficients a_1 through a_9 and initial conditions subject to the constraints in Eq. (4) did not reveal any bounded solutions with a largest Lyapunov exponent greater than 0.001. Thus it seems likely that system (1) does not admit chaotic solutions in the presence of such a fully unstable equilibrium.

Therefore, inspired by the Sprott A (Nose–Hoover) system [18–20], and using a form that has successfully given other chaotic flows with hidden attractors [1,2,5], system (1) was modified slightly according to

$$\dot{x} = y$$
$$\dot{y} = -x + yz$$
$$\dot{z} = a_1x + a_2y + a_3z + a_4x^2 + a_5y^2 + a_6xy + a_7xz + a_8yz + a_9 \tag{5}$$

System (5) has only one equilibrium point at $(0, 0, -a_9/a_3)$ with eigenvalues λ that satisfy

$$\lambda^3 - \left(a_3 - \frac{a_9}{a_3}\right)\lambda^2 + (-a_9 + 1)\lambda - a_3 = 0 \tag{6}$$

Changing the variable $\lambda \to -\lambda$ gives

$$\lambda^3 + \left(a_3 - \frac{a_9}{a_3}\right)\lambda^2 + (1 - a_9)\lambda + a_3 = 0 \tag{7}$$

The Routh–Hurwitz stability criterion guarantees that the real part of all eigenvalues are positive provided

$$\left(a_3 - \frac{a_9}{a_3}\right) > 0$$
$$\left(a_3 - \frac{a_9}{a_3}\right)(1 - a_9) - a_3 > 0$$
$$a_3 > 0 \tag{8}$$

For this case, many chaotic solutions were found in an extensive computer search, although they are still relatively rare. Perhaps the simplest such system [21] is given by

$$\dot{x} = y$$
$$\dot{y} = -x + yz$$
$$\dot{z} = z + ax^2 - y^2 - b \tag{9}$$

with an appropriate choice of the parameters a and b and initial conditions. System (9) satisfies the conditions of Eq. (8) provided $b > 0$. With seven terms, this is actually a three-parameter system, but for simplicity, the third parameter is taken as unity. The remainder of the paper is concerned with the properties of system (9).

3. Equilibrium properties

By design, this system (9) has only one equilibrium at $(0, 0, b)$ with eigenvalues λ given by

$$\lambda^3 - (b+1)\lambda^2 + (b+1)\lambda - 1 = 0 \tag{10}$$

whose roots are $\lambda = 1$, $b/2 \pm \sqrt{b^2 - 4}$. Since one of the eigenvalues is $+1$, the equilibrium is always unstable, but the type of equilibrium depends on b and is independent of a as summarized in Table 1 where $\Delta = b^2 - 4$ and $\omega = \sqrt{4 - b^2}$.

Chaotic solutions occur for $b > 1$ and are most abundant at large b where the equilibrium is an unstable node. For a typical value of $b = 4$, the eigenvalues are $\lambda_1 = 3.732050808$, $\lambda_2 = 1$, $\lambda_3 = 0.267949192$, and the corresponding eigenvectors are

$$\mathbf{v}_1 = \pm(k_x + 3.732050808k_y)$$
$$\mathbf{v}_2 = \pm k_z$$
$$\mathbf{v}_3 = \pm(k_x + 0.267949192k_y) \tag{11}$$

Table 1
Types of equilibrium points for different values of the parameter b.

Parameter b	Eigenvalues	Type of equilibrium point
$b < -2$	$1, (b \pm \sqrt{\Delta})/2$	saddle node
$-2 < b < 0$	$1, (b \pm i\omega)/2$	saddle focus
$0 < b < 2$	$1, (b \pm i\omega)/2$	unstable focus
$b > 2$	$1, (b \pm \sqrt{\Delta})/2$	unstable node

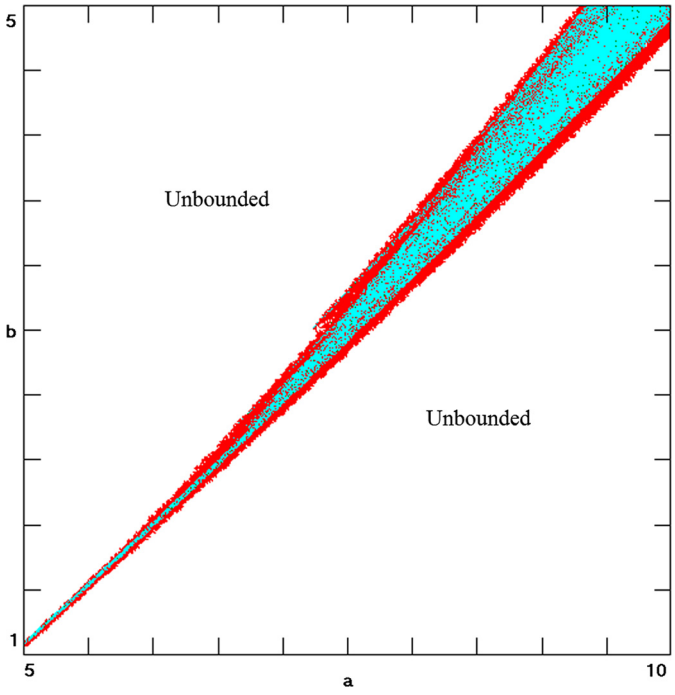

Fig. 1. Regions of various dynamical behaviors for system (9) as a function of the bifurcation parameters a and b. The chaotic regions are shown in red, the periodic (limit cycle) and quasiperiodic (torus) regions are shown in blue, and the unbounded regions are shown in white. (For interpretation of the references to color in this figure legend, the reader is referred to the web version of this article.)

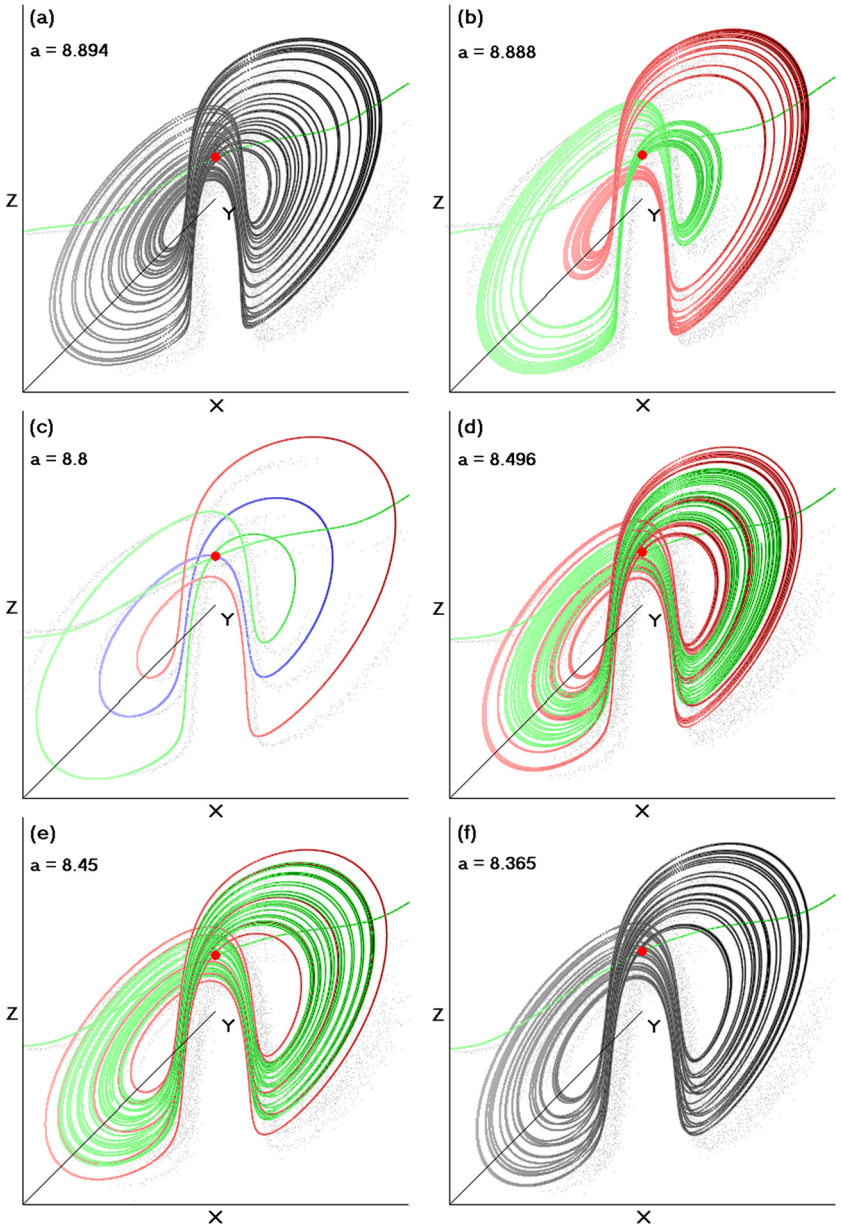

Fig. 2. Chaotic attractors from Eq. (9) for $b = 4$ at various values of a. The unstable node is shown as a red dot along with its most unstable manifold in green. See Table 2 for more detail. (For interpretation of the references to color in this figure legend, the reader is referred to the web version of this article.)

where k_x, k_y, and k_z are unit vectors in the x, y, and z directions, respectively. These vectors define the unstable manifolds in the vicinity of the equilibrium point and are independent of the parameter a.

4. Dynamic regions and bifurcations

Most of the solutions of system (9) are unbounded, but there is a narrow triangular region in the vicinity of the line $b = 0.8a - 3$ where periodic and chaotic solutions occur as shown in Fig. 1. For each (a, b) combination in this plot, it was necessary to search for initial conditions that give bounded solutions and then test whether the solution is periodic or chaotic by calculating the largest Lyapunov exponent. The chaotic regions indicated in red have a largest Lyapunov exponent greater than 0.001. Some of the periodic solutions indicated in blue with Lyapunov exponents close to zero are actually quasiperiodic with an attracting torus. Furthermore, there are regions of multistability where there are coexisting attractors as will be discussed shortly and that accounts for the mingling of red and blue dots in some regions of the plot. Note that bounded solutions only occur for $b > 1$ and are most prominent at large b. There is some uncertainty in the results because the Lyapunov exponent can converge slowly, but the qualitative features should be correct.

For the system to have attractors, the state space contraction given by $1 + \langle z \rangle$ must be negative, or $\langle z \rangle < -1$, where $\langle z \rangle$ is the time-averaged value of z along the orbit. Furthermore, since the system is rotationally symmetric under the transformation $(x, y, z) \to (-x, -y, z)$, any attractors are either symmetric under a 180° rotation about the z-axis or there is a symmetric pair of them.

As indicated in Fig. 1, most of the qualitative behavior is captured by varying a over a narrow range with b fixed at a value chosen as $b = 4$. Fig. 2 shows a variety of different attractors that occur with their properties summarized in Table 2.

Table 2
Details of the attractors shown in Fig. 2.

Figure	Parameter ($b = 4$)	Initial conditions	Lyapunov exponents	Kaplan–Yorke dimension	Attractor type
2(a)	$a = 8.894$	(0, 3.8, 0.7)	0.1767 0 −0.9158	2.1929	Symmetric strange attractor
2(b)	$a = 8.888$	(1, −2, 4) (−1, 2, 4)	0.1642 0 −1.1189	2.1468	Symmetric pair of strange attractors
2(c)	$a = 8.8$	(1, 7, −9.5) (−1, −7, −9.5)	0 −0.4116 −0.4116	1.0	Symmetric pair of limit cycles
2(c)	$a = 8.8$	(1.518, 0.488, −6)	0 −0.0056 −0.0056	1.0	Symmetric limit cycle
2(d)	$a = 8.496$	(0.09, 7.6, 0)	0 0 −0.0370	2.0	Symmetric attracting torus
2(d)	$a = 8.496$	(0, 4.4, 0.65)	0.0476 0 −0.2632	2.1807	Symmetric strange attractor
2(e)	$a = 8.45$	(1.46, 0, 0.1)	0 −0.0810 −0.0810	1.0	Symmetric limit cycle
2(e)	$a = 8.45$	(0, 5.6, 0.86)	0 0 −0.0438	2.0	Symmetric attracting torus
2(f)	$a = 8.365$	(0, −5, 0.8)	0.0403 0 −0.0896	2.4498	Symmetric strange attractor

Fig. 3 shows the Lyapunov exponents (LEs), Kaplan–Yorke dimension (Dky), and the maximum values of x (Xm) for $8.8 < a < 8.9$ and $b = 4$. At small a, there is a symmetric pair of limit cycles that undergo a period-doubling route to chaos and then continue to grow, with periodic windows, until they merge into a single symmetric strange attractor at $a = 8.89$, which is destroyed in a boundary crisis at $a = 8.895$.

The behavior of the system at smaller values of the parameter a is shown in Fig. 4. As a is decreased from 8.8, the symmetric pair of limit cycles is destroyed in a discontinuous bifurcation around $a = 8.77$, and a symmetric limit cycle appears and gives birth to a thin attracting torus at $a = 8.72$, which is unusual in a three-dimensional system. The torus grows in size, with small periodic windows, until it is destroyed in a discontinuous bifurcation around $a = 8.44$, and a new symmetric limit cycle appears that abruptly vanishes around $a = 8.35$.

5. Multistability

Already mentioned is the symmetric pair of limit cycles that period-double into the symmetric pair of strange attractors shown in Fig. 2(b). This is an example of symmetry breaking in which the symmetric equations produce a symmetric pair of asymmetric attractors.

The discontinuous bifurcations that are evident in Fig. 4 suggest hysteresis and bistability as confirmed by Fig. 5 which is the same as Fig. 4 except that a is slowly increased from 8.35 without reinitializing. The regions of multistability are clearly evident when the two figures are compared. In particular, the pair of limit cycles that appears in Fig. 4 at $a = 8.8$ is accompanied by a symmetric limit cycle indicated in Fig. 5, and the three coexisting limit cycles are shown in Fig. 2(c).

Furthermore, there is a small region near $a = 8.496$ where there is a symmetric strange attractor as evidenced by the positive Lyapunov exponent in Fig. 5(a). This symmetric strange attractor coexists with a symmetric attracting torus as evidenced by the zero Lyapunov exponent at the same value of a in Fig. 4(a), and the two attractors are strongly intertwined as seen in Fig. 2(d). The coexistence of a strange attractor and attracting torus in a 3-D system with quadratic nonlinearities is surely unusual, and this may be the first such reported example.

In the vicinity of $a = 8.45$, Fig. 5 shows a limit cycle while Fig. 4 shows a torus. The two attractors are intertwined as shown in Fig. 2(e). The limit cycle undergoes period doubling, leading to the strange attractor just described, all the while coexisting and intertwined with an attracting torus. A cross section of the basins of attraction in the $x = 0$ plane at $a = 8.496$ is shown in Fig. 6. The basin of the strange attractor (in red) is nested within the basin of attraction of the torus (in blue), which itself occupies a small fraction of the space of initial conditions. These behaviors are surely unusual. Whether they have anything to do directly with the presence of the unstable node is an open question worthy of further study.

Finally, there is a region near $a = 8.65$ in Fig. 5 where another narrow band of chaos occurs with a symmetric strange attractor having a relatively large Kaplan–Yorke dimension of 2.4498 and shown in Fig. 2(f). All of the attractors have a similar shape presumably because they occur nearby in parameter space.

6. Hidden attractors

Recent research has involved categorizing periodic and chaotic attractors as either self-excited or hidden [11–17]. A self-excited attractor has a basin of attraction that is associated with an unstable equilibrium, whereas a hidden attractor has a basin of attraction that does not intersect with small neighborhoods of any equilibrium points. The classical attractors of Lorenz, Rössler, Chua, Chen, Sprott systems (cases B to S) and other widely-known at-

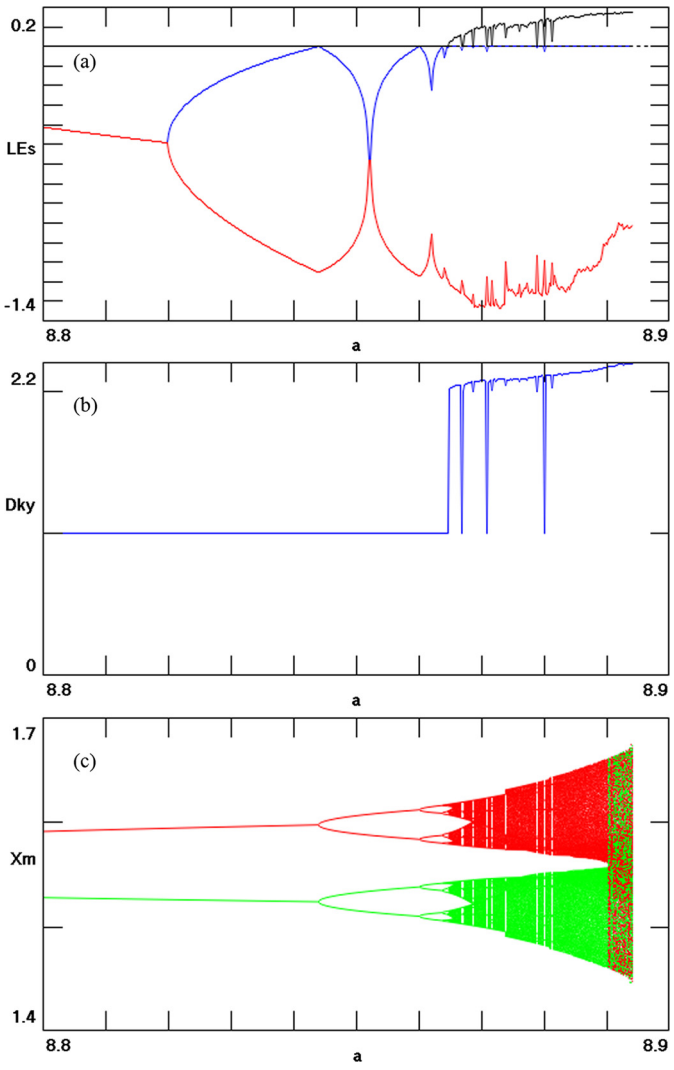

Fig. 3. (a) Lyapunov exponents, (b) Kaplan–Yorke dimension, and (c) maxima of x for system (9) versus a with $b = 4$.

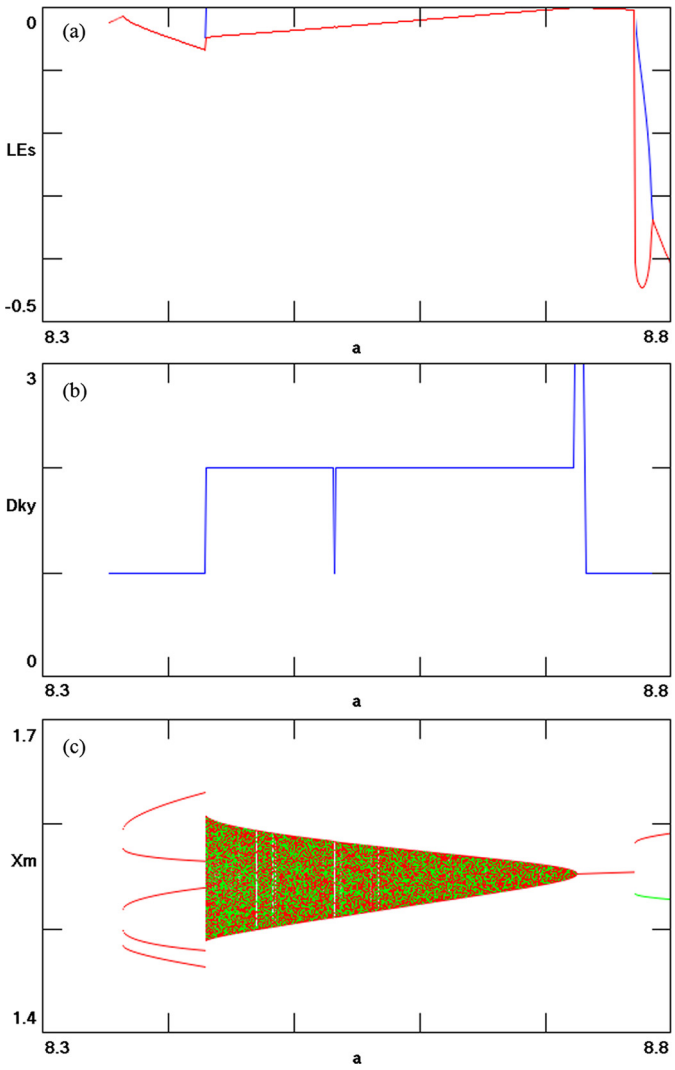

Fig. 4. (a) Lyapunov exponents, (b) Kaplan–Yorke dimension, and (c) maxima of x for system (9) versus a with $b = 4$. In this plot, a is slowly decreased from 8.8 without reinitializing.

tractors are those excited from an unstable equilibrium. From a computational point of view this allows one to use a numerical method in which a trajectory started from a point on the unstable manifold in the neighborhood of an unstable equilibrium, reaches an attractor and identifies it [15]. Hidden attractors cannot be found by this method and are important in engineering applications.

As a test of whether the attractors described here are hidden, initial conditions were chosen on the most unstable manifold given by the vector $\mathbf{v}_1$ in Eq. (11) using values of (± 0.001, ± 0.003732050808, 4) close to the node. The subsequent trajectories as shown in green in Fig. 2 diverge toward infinity and do not approach any of the attractors. Furthermore, three cross sections of the basin of attraction for the strange attractor with $a = 8.894$, $b = 4$ that intersect the unstable node are shown in Fig. 7, where it appears that the basin comes nowhere near the equilibrium point. The small size of the attractor basin along with the narrow region of parameter space shown in Fig. 1 illustrate why this chaotic system was hard to find, and this may be a general feature of chaotic systems with unstable nodes.

As an additional test of whether the attractors are hidden, a hundred thousand Gaussian random initial conditions were chosen centered on the equilibrium with a variance of 0.001, and they all diverged toward infinity. Finally, another hundred thousand initial conditions were chosen randomly on the strange attractor and followed backward in time so that the attractor becomes a repellor, and none of the resulting trajectories approached a small neighborhood of the node, which is stable in reversed time with a relatively large basin of attraction. Hence we conclude that these attractors are hidden by any of the means usually used to find them.

7. Conclusion

A very rare three-dimensional quadratic flow has been reported here in which periodic, quasiperiodic, and chaotic attractors coexist with a single unstable node. It was found by carefully designing a system to have a single equilibrium whose eigenvalues have only positive real parts and then numerically searching the resulting space of nine parameters and three initial conditions for chaotic solutions. This system has unusual properties including symmetry breaking, attractor merging, attracting tori, and various types of multistability. Numerical evidence shows that these attractors are hidden and hence represent a new class of hidden attractor. It

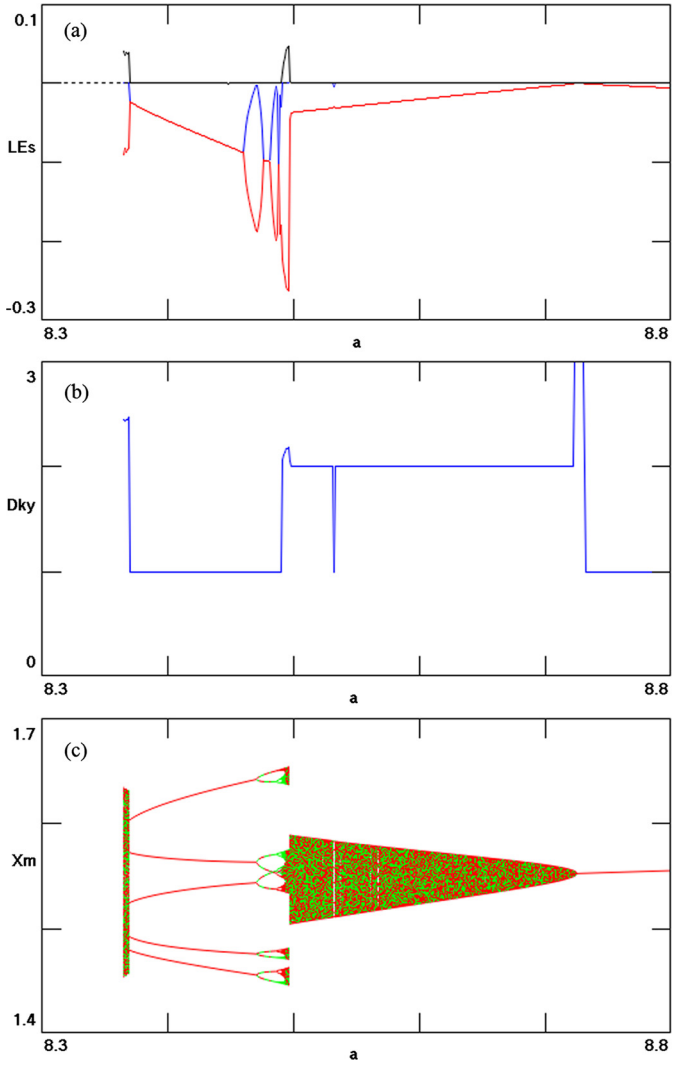

Fig. 5. (a) Lyapunov exponents, (b) Kaplan–Yorke dimension, and (c) maxima of x for system (9) versus a with $b = 4$. In this plot, a is slowly increased from 8.35 without reinitializing.

may be the simplest system with this combination of characteristics, although it could be generalized by adding a third bifurcation parameter.

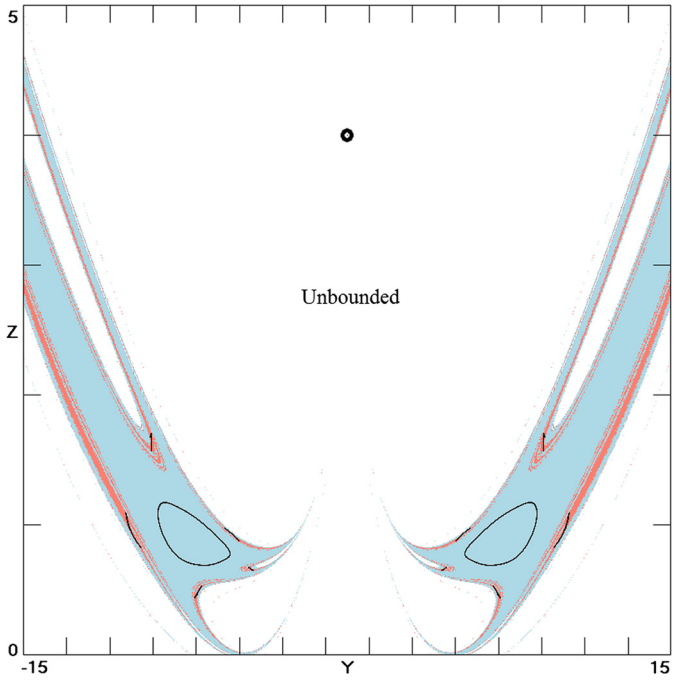

Fig. 6. Cross section in the $x = 0$ plane of the basins of attraction for $a = 8.496$ and $b = 4$. The blue area is the basin of the torus, the red area is the basin of the strange attractor, and unbounded regions are shown in white. Cross sections of the attractors are shown in black, and the unstable equilibrium is shown as a small circle at the center toward the top. (For interpretation of the references to color in this figure legend, the reader is referred to the web version of this article.)

Acknowledgement

We thank Professor Seyed Mohammad Reza Hashemi Golpayegani for support and help which enhanced the quality of the paper.

References

[1] S. Jafari, J. Sprott, Chaos Solitons Fractals 57 (2013) 79–84.
[2] S. Jafari, J. Sprott, S.M.R.H. Golpayegani, Phys. Lett. A 377 (2013) 699–702.
[3] S. Kingni, S. Jafari, H. Simo, P. Woafo, Eur. Phys. J. Plus 129 (2014) 1–16.
[4] S.-K. Lao, Y. Shekofteh, S. Jafari, J.C. Sprott, Int. J. Bifurc. Chaos 24 (2014).
[5] M. Molaie, S. Jafari, J.C. Sprott, S.M.R.H. Golpayegani, Int. J. Bifurc. Chaos 23 (2013).
[6] V.-T. Pham, S. Jafari, C. Volos, X. Wang, S.M.R.H. Golpayegani, Int. J. Bifurc. Chaos 24 (2014).

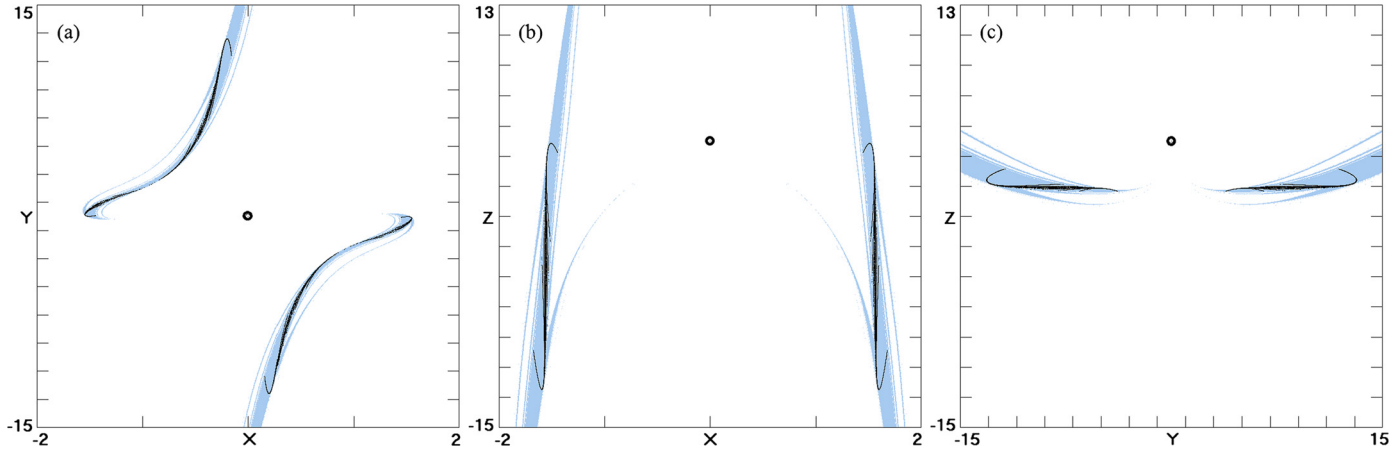

Fig. 7. Cross sections of the basin of attraction of the strange attractor at $a = 8.894$ and $b = 4$ in the planes (a) $z = b$, (b) $y = 0$, and (c) $x = 0$. Cross section of the strange attractor is shown in black, and the unstable equilibrium is shown as a small circle.

[7] V.-T. Pham, C. Volos, S. Jafari, Z. Wei, X. Wang, Int. J. Bifurc. Chaos 24 (2014).
[8] X. Wang, G. Chen, Commun. Nonlinear Sci. Numer. Simul. 17 (2012) 1264–1272.
[9] X. Wang, G. Chen, Nonlinear Dyn. 71 (2013) 429–436.
[10] Z. Wei, Phys. Lett. A 376 (2011) 102–108.
[11] V. Bragin, V. Vagaitsev, N. Kuznetsov, G. Leonov, J. Comput. Syst. Sci. Int. 50 (2011) 511–543.
[12] G. Leonov, N. Kuznetsov, J. Math. Sci. 201 (2014) 645–662.
[13] G. Leonov, N. Kuznetsov, M. Kiseleva, E. Solovyeva, A. Zaretskiy, Nonlinear Dyn. 77 (2014) 277–288.
[14] G. Leonov, N. Kuznetsov, O. Kuznetsova, S. Seledzhi, V. Vagaitsev, Trans. Syst. Control 6 (2011) 54–67.
[15] G. Leonov, N. Kuznetsov, V. Vagaitsev, Phys. Lett. A 375 (2011) 2230–2233.
[16] G. Leonov, N. Kuznetsov, V. Vagaitsev, Phys. D, Nonlinear Phenom. 241 (2012) 1482–1486.
[17] G.A. Leonov, N.V. Kuznetsov, Int. J. Bifurc. Chaos 23 (2013).
[18] W.G. Hoover, Phys. Rev. E 51 (1995) 759.
[19] H.A. Posch, W.G. Hoover, F.J. Vesely, Phys. Rev. A 33 (1986) 4253.
[20] J. Sprott, Phys. Rev. E 50 (1994) R647.
[21] J.C. Sprott, Elegant Chaos: Algebraically Simple Chaotic Flows, World Scientific, 2010.